Available online at www.sciencedirect.com

ScienceDirect

Procedia CIRP 110 (2022) 208–213

www.elsevier.com/locate/procedia

V CIRP Conference on Biomanufacturing

A feasibility analysis of a 3D customized upper limb orthosis

Francesca Sala[a]*, Mattia Carminati[a], Gianluca D'Urso[a], Claudio Giardini[a]

[a]Department of Management, Information and Production Engineering – University of Bergamo, via Pasubio 7/b, 24044 Dalmine (BG), Italy

* Francesca Sala. *E-mail address:* francesca.sala@unibg.it

Abstract

Additive Manufacturing (AM), also known as 3D printing, is considered one of the most advanced and innovative production technologies. Given the possibility to realize tailor-made and complex geometries compared to conventional processes, the medical industry demonstrated a considerable interest towards these topics. In particular, leveraging on AM technologies, orthopedy is the field able to achieve greater benefits, prototyping components characterized by improved design and comfort of use. As a result, to display the benefits of the AM technologies deployment in clinical practice, the present work was developed, proposing an alternative procedure to manufacture customized upper limb orthosis via 3D printing. The suggested methodology involved a fast and accurate 3D scanning of the hand-wrist-arm district to obtain the surface anatomy of the patient. A Graphical User Interface (GUI), integrating a series of semi-automatic commands to model the medical device starting from the 3D shape point cloud, was built. The limb orthosis obtained using the proposed system was manufactured by means of biocompatible filaments (ABS) and a Fused Deposition Modelling (FDM) printer. Furthermore, a time-cost assessment was carried out tailored to the developed medical application. Results demonstrated that the AM techniques might provide a valid technical and cost-effective alternative to the traditional fabrication methods.

Keywords: Additive manufacturing; 3D printing; FDM; limb orthosis; graphical user interface; cost model.

1. Introduction

Additive Manufacturing (AM), also known as 3D printing, is considered one of the most advanced and innovative production technologies. In recent years, the availability of accessible techniques and biocompatible materials promoted a significant deployment of these methodologies in the medical industry and, in particular, in the orthopaedic field [1,2] with the prototyping of customized prostheses and orthoses [3].

Traditional manufacturing techniques of tailor-made orthoses are based on vacuum forming and the use of low-temperature thermoplastic (LTT) materials, both of which require close contact with the patient's limb and are highly dependent on the skills and experience of the health care operator [4,5]. The medical devices resulting from such procedures are often unsatisfactory in terms of comfort, causing complications (e.g., cutaneous diseases, compartment syndromes, bone and joint injuries) and difficulties in patient adherence to the clinical prescription [6]. Several studies [7–10] successfully addressed these issues by exploring different methodologies to re-engineer medical devices for the treatment of acute conditions affecting the joints and bones of the hand-wrist-arm district. Nonetheless, these approaches partially or completely lack a rapid, automated and consistent system for modelling orthosis. The present study fits into this framework proposing a standardized and guided procedure for the fabrication of customized upper limb orthoses for the treatment of chronic and non-acute illnesses via reverse engineering and AM. The study is supplemented with a feasibility analysis, including an assessment of the time and cost of the implementation of the new methodology within the clinical framework.

10.1016/j.procir.2022.06.038

The present work renews the traditional manufacturing techniques of orthotic devices, making them extremely customized, repeatable and cost-effective. The delivered medical solutions are intended to treat those conditions defined as non-acute and long-term, overcoming the drawbacks related to the comfort and functionality of conventional orthoses.

2. Methodology

2.1. Scanning Operation

The high-speed acquisition is a fundamental operation for accurate orthosis scanning since, during the entire procedure, the patient needs to stand still in the same position for an extended period. The optimal set-up is represented by the patient sat down with the arm lifted frontally at the height of the shoulder joint. A support was placed under the middle phalanxes and the thumb was kept separately from the hand. The acquisition of the 3D shape was performed by means of the Hexagon Absolute Arm 7-Axis equipped with RS5 Laser Scanner (Figure 1).

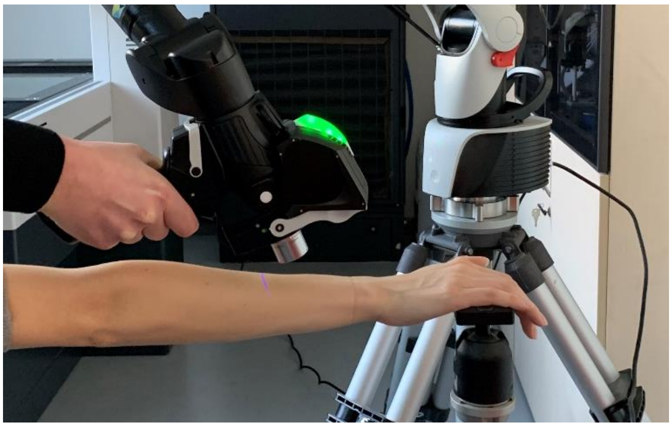

Figure 1. Optimal configuration of the 3D limb geometry acquisition with the Hexagon Absolute Arm 7-Axis equipped with RS5 Laser Scanner.

The scanning procedure was preceded by preliminary operations accomplished with Polyworks Inspector. A clipping plane, useful to delimit the region of interest, was defined using a 6 mm touching probe. A point cloud was selected as extraction data type and a standard resolution was chosen since details smaller than 1 mm in size were not required for this kind of scan model. Then, a single 360° scansion around the patient's arm was acquired.

2.2. Surface elaboration

With PolyWorks Modeler, the digitized point cloud was transformed into a surface-based polygonal model, which is more accurate and less noisy. Automatically, the modeler recognizes and resolves the most evident topological errors and reconstructs the mesh fixing the surface triangulation. All the gaps and holes with a diameter lower than a target value were individually closed and all the detached elements were removed manually. The success of the described procedure is strictly compliant with the software design ability of the operator.

The .STL file was exported to a commercial CAD software, where the limb surface-based model was manually processed into an orthotic solid-based model. Given the absence of a specific orientation in the exported model, the limb surface was aligned in a defined coordinate system. A smoothing action was applied to the limb surface and two offsets were generated. The first creates the 3D solid geometry, while the second ensures sufficient ease between the arm and the orthosis. Cut operations were applied to the orthosis extremities to preserve the shape of interest. A parametric pattern of holes was included to lighten the structure and the model was divided into two shells along the arm centre line.

2.3. CAD modelling

The procedure described in Section 2.2 is inconsistent with the time and cost required by the clinical necessity of realizing orthoses. Besides, the process is strictly connected with the ability of the operators to model the scanned point cloud into a printable .STL file. Such issues generate the need to develop a proper automated system to shorten the time procedure and ease the clinical staff during the creation of the limb device. A CAD modelling system was designed and it was conceived as a simple and straightforward Graphical User Interface (GUI), composed of different commands that produce an accurate .STL model of the orthosis from the 3D scanned forearm. Python language libraries such as PyQt5, Vtk and PyMeshLab were involved to automate the CAD modelling process.

The new modelling procedure requires the polygonal model to be loaded in the GUI workspace. As opposed to the procedure described in Section 2.2, the operations leading to the generation of an orthopaedic model are uniformed and automated through the creation of functions, integrating different algorithms.

The function *fix_mesh* translates the model to the origin of the global reference system created in the environment and removes duplicated vertices and faces. The *Quadric Edge Collapse Decimation* algorithm simplifies the number of triangles in the textured mesh. The *Ball Pivoting* algorithm reconstructs surfaces using existing points without creating new ones. All the detached points are deleted and holes with diameters up to a defined measure are closed.

The function *smooth_mesh* enhances the surface of the model leveraging on the *Laplacian Smooth* feature, which is iterated with a sufficiently low number of repetitions to prevent mesh degeneration.

After the levelling operation, the function *expand_mesh* creates an offset towards the outside of the surface model, fulfilling both the wearability and the immobilization aspects of the orthotic device.

The function *hollow_mesh* creates a new mesh, which is a resampled version of the current one, using the *Marching Cube* algorithm that generates a solid shape with a customizable thickness.

The function *rotate_mesh* is responsible for the arbitrary rotation of the solid along the three Cartesian coordinates. This operation is exploited in conjunction with the function *crop_mesh*, utilized to remove the useless anatomic regions of the orthosis. Both operations are kept manually allowing the clinical staff to adjust the most critical anatomical areas.

The orthotic structure is emptied via ventilation holes, by means of the function *addholes_mesh*. The procedure necessitates the execution of a Boolean difference between two meshes, the current one and the one representative of the gaps shape. A library containing different holes designs is available and their actual positioning is performed manually at the discretion of the specific clinical case.

Furthermore, the *clamp_mesh* function manages the arbitrary insertion of the fastening systems, designed to join the two shells of the orthopedic orthosis. The operation consists of a Boolean union among the current orthosis meshes and the joint system mesh (selected from a dedicated library).

Finally, the function *fork_mesh* divides the model into two orthotic shells, generating two .STL files, each representing a half of the orthosis.

2.4. Additive Manufacturing

The customized orthosis can be realized using Fused Deposition Modelling (FDM), which represents the perfect technique considering the complex shape of an orthotic device and its required fabrication cost and time.

The manufacturing process was realized using an Ultimaker S5 machine equipped with a head nozzle of 0.8 mm extruding an ABS (Acrylonitrile Butadiene Styrene) filament as the primary material to realize the printed orthosis. ABS was chosen according to factors, including biological compatibility. Given the alleged purposes and, in accordance with the standard [11], the materials required to be compatible only in terms of cytotoxicity, sensitization and irritation (or intracutaneous reactivity). Considerable attention was paid to the aspects of ease of printing and low purchase cost of materials. Ultimaker Breakaway was selected as the support material since it can be removed easily and manually from the orthosis after the end of the printing process.

The selected printing parameters of the ABS filament are a 250°C nozzle temperature and a printing speed of 60 mm/s. A layer height of 0.6 mm ensures a considerable time reduction of the printing process. The infill density rate was set to 100%.

The Ultimaker Cura 3D printing software was used to prepare the model and generate the G-code file to print.

2.5. Cost model

Based on existing cost assessments and valuations found in the literature [12,13], a comprehensive model for estimating the manufacturing costs of an AM orthosis was formulated. The parameters, included in the analysis, comprise the 3D printing (P) and 3D scanner (S) purchase costs and the costs related to their power consumption (E), the manufacturing material costs (M) and operator labour costs (L).

As shown in Eq. 1, P parameter was calculated as the product of the entire production time (Tp) and the purchase cost (Pp) standardized over its useful operating time, given by the utilization rate (Kp) and useful life (Yp) of the technology. In particular, Tp corresponds to the deposition time (Td) plus non-deposition times (Tnd) or other times related to pre-print and post-print preparation (warm-up (Twu), set-up (Tsu) and cooling (Tc) times).

$$P = \frac{T_p \times P_p}{K_p \times Y_p} \qquad \text{Eq. 1}$$

The preceding mathematical expression was suitably modified to define S factor, as presented in Eq. 2. The scanning time (Ts) is a single component, directly assessed during the arm measurement activity.

$$S = \frac{T_s \times P_s}{K_s \times Y_s} \qquad \text{Eq. 2}$$

As shown in Eq. 3, E parameter is the energy consumption cost related to the 3D printing and 3D scanner technologies. Particularly, Pe stands for the cost of electricity and Ci for the power consumption measured during specific time intervals Ti (where $i = \{Td; Tnd; Ts\}$).

$$E = P_e \times (T_d \times C_{Td} + T_{nd} \times C_{Tnd} + T_s \times C_{Ts}) \qquad \text{Eq. 3}$$

The M factor depends on the characteristics of the two extruded elements, the material (m) and the support material (ms). As displayed in Eq. 4, the parameters involved in the calculations are infill percentage (in), component volume (V), material density (ρ) and material cost (P). Specifically, Vm and Vms were derived from the values of the extruded wire length multiplied by the wire section surface.

$$M = in_m \times (\rho_m \times V_m \times P_m) + in_{ms} \times (\rho_{ms} \times V_{ms} \times P_{ms}) \qquad \text{Eq. 4}$$

Lastly, Eq. 5 expresses the cost of labour parameter (L), simply given by the product of the hourly wage (Pl) and the working time (Tl) of the operator.

$$L = T_l \times P_l \qquad \text{Eq. 5}$$

The overall cost to produce an AM orthosis is determined by the sum of the previous five equations as reported in Eq. 6.

$$C_{AM\ orthosis} = P + S + E + M + L \qquad \text{Eq. 6}$$

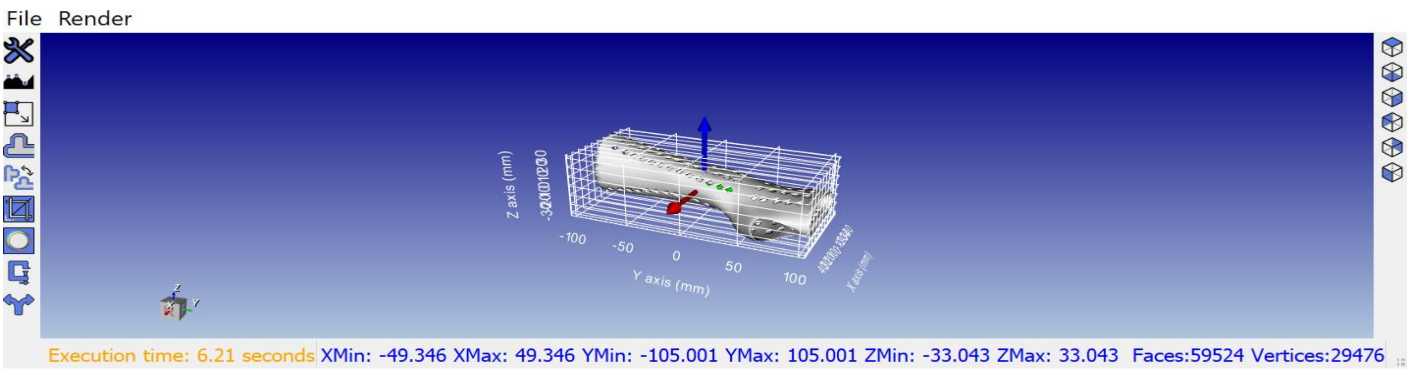

Figure 2. GUI.

3. Results

3.1. Scanning procedure and CAD modelling

The contactless acquisition of the arm shape, accomplished by an experienced operator following the procedure described in Section 2.1, took slightly less than 2 min (Table 1).
The developed GUI (Figure 2) is organized into five areas: menu, view bar, status bar, workspace and task bar. The menu (upper area) handles actions related to file management, such as uploading and saving the file. The view bar (right area) allows to interact with the virtual camera and display the object from different perspectives. The status bar (bottom area) shows real-time information such as the execution time of the current operation, the coordinates and the number of faces and vertices of the model. The workspace (central area) represents the environment in which the polygonal model is processed. The generation of the final orthotic model is accomplished by nine primary commands reported in the operations bar (left area): model translation and pre-adjustment, surface smoothing, solid generation, rotation, cutting, ventilation holes creation, fastening systems implementation and model partitioning.
Orthotic modeling operations are summarized in Table 1. The first operations that were performed on the limb scan concerned its translation in the workspace origin and the optimization of the mesh (e.g., the closure of holes with diameter less than 50mm). During surface smoothing, the Laplacian algorithm was iterated 50 times to avoid mesh degeneration. Two adjustable offsets were created: the first offset of 2 mm eases orthotic wearability, the second offset between 2-4 mm corresponds to the thickness generating the solid. The cutting operation, along with the rotation function, removed the upper and lower extremities and refined the area around the thumb. The orthotic solution was characterized by a ventilated structure, lightening the device and providing easy access to rehabilitative therapies (e.g., electrostimulation). Holes of rhomboidal shapes were selected to prevent material collapse during deposition, minimizing support material usage to surface overhangs only and speeding up the time required for the support removal. In the present model, four rows of holes (spaced 10 mm apart) were introduced in the areas of the hand and forearm. Ultimately, the orthotic model was divided into two complementary shells joined by 12 fastening systems (6 per shell) enabling quick removability during medical inspection of the injured area.

Table 1. Scanning procedure and operations for generating an orthotic model.

Scanning procedure and modelling steps		Time and std [s]
	Acquisition of a single 360° scansion around the patient's arm	110.0
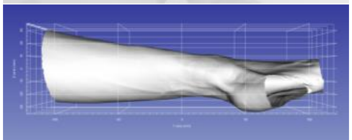	Primary processing (translation and pre-adjustment)	9.43 ± 0.05
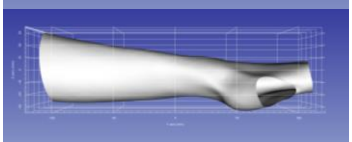	Surface smoothing	0.73 ± 0.01
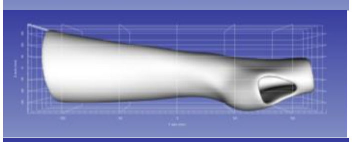	Offset creation	48.67 ± 0.38
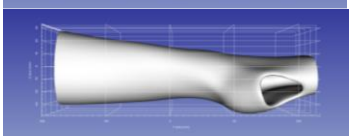	Rotation and cutting	3.94 ± 0.73
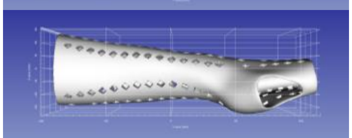	Creation of ventilation holes	737.31 ± 50.31
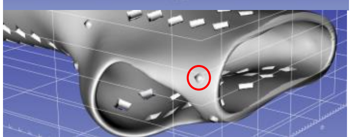	Implementation of fastening systems	63.92 ± 10.72
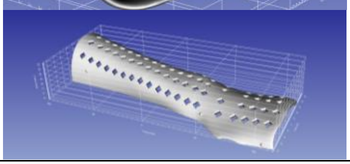	Model partitioning into two shells	2.23 ± 0.59

The times of the operations to generate a new orthotic model via GUI are reported in Table 1. Standard deviations, computed on the execution of three tests, are provided as an indication of repeatability and reproducibility of the developed modelling system. The GUI procedure lasts approximately 15 min, reducing the elaboration times compared to the manual modeling executed by a CAD expertise (this one lasting more than 2.5 h).

3.2. Orthosis fabrication

For the creation of the orthosis prototype (Figure 3), 85.5 cm^3 of ABS material was used. 1.04 cm^3 of support material was added for an angle of overhangs greater than 88°. This angle allows to reduce to a minimum the consumption of the support material, placed in correspondence of the upper zone of the hand, and simultaneously to provide the correct realization of the product. The finishing treatment was performed, since the aim of the study was the feasibility analysis of an orthosis device realized with a semi-automated process.

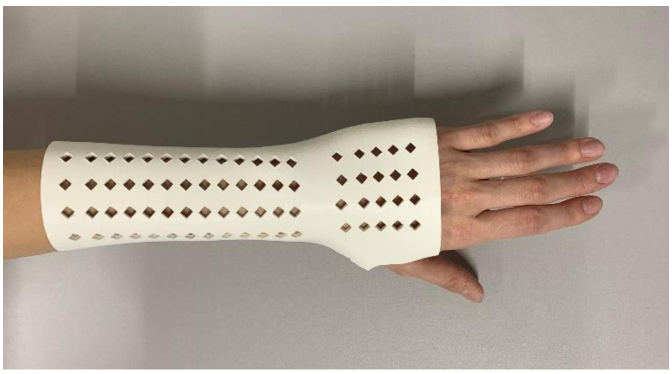

Figure 3. Early prototype of the limb orthosis.

As reported in Section 2.4, a layer height of 0.6 mm was selected to lower the deposition time. Tensile tests [14] and three point bending tests [15] were carried out to verify a possible inverse relationship between the layers height of the samples and their mechanical properties. For each test, three samples with 0.1 mm layer height and three samples with 0.6 mm layer height were printed.

An analysis of variance (ANOVA) was performed and Table 2 reports the p-value obtained after the ANOVA. It is possible to observe that the layer height affected both the tensile and flexural strengths of the samples. Moreover, the layer height of 0.6 mm ensured higher levels of tensile and flexural strength (Table 3).

Table 2. Influence of the layer height on the tensile and flexural strength.

	p-value	
	Tensile strength	Flexural strength
Layer height	0.000	0.016

Table 3. Mean tensile and flexural strength as a function of the layer height.

	Layer height [mm]	
	0.1	0.6
Mean tensile strength [MPa]	31.3	39.5
Mean flexural strength [MPa]	85.1	96.8

3.3. Time-cost evaluation

Table 4 provides a view of the main parameters contributing to the 3D printing cost, which amounts to 0.60 €. *Tp* was derived from two contributions. The deposition time (1.92 h) resulted from a 3D printer slicing program and it was dependent on the complexity of the .STL file and the printing process parameters (e.g., layer height, layer width, printing speed). The non-deposition times, including warm-up (0.12 h), set-up (0.03 h) and cooling (0.13 h) times, were dependent on the properties of the selected material.

Table 4. 3D printing parameters and cost.

Parameter	Symbol [unit]	Value
Production time	*Tp* [h]	2.20
Technology purchase cost	*Pp* [€]	6,000.00
Technology deployment	*Kp* [1]	0.50
Technology useful life	*Yp* [y]	5.00
3D printing cost	*P* [€]	0.60

The cost of the 3D scanner is 0.24€ per orthoses, as shown in Table 4.

The energy cost depends entirely on the 3D printer parameters and resulted to be 0.14 €. The non-deposition phase is responsible for both nozzle and build plate heating and, consequently, requires higher power supply values than the actual deposition phase. On the other side, the scanner energetic contribution can be considered negligible. The power supply parameters *Ctp*, *Ctnp*, and *Cts* were all measured with an electricity consumption sensor and are displayed in Table 6.

Table 5. 3D scanner parameters and cost.

Parameter	Symbol [unit]	Value
Scanning time	*Ts* [h]	0.03
Scanner purchase cost	*Ps* [€]	70,000.00
Scanner deployment	*Ks* [1]	0.10
Scanner useful life	*Ys* [y]	10.00
3D scanner cost	*S* [€]	0.24

Table 6. Energy parameters and cost.

Parameter	Symbol [unit]	Value
Electricity cost	*Pe* [€/kWh]	0.26
Technology power consumption during *Tp*	*Ctp* [kW]	0.23
Technology power consumption during *Tnp*	*Ctnp* [kW]	0.31
Scanner power consumption	*Cts* [kW]	0.19
Energy cost	*E* [€]	0.14

The parameters of material cost are shown in Table 7. The volume of a component was derived from the information on the wire area and the extruded wire length, obtained from the 3D printer slicing program. The extruded wire lengths were 13.51 m for the ABS and 0.16 m for the Breakaway. The overall material cost is 4.71 € while the cost of the support material is negligible.

Table 7. Material parameters and cost.

Parameter	Symbol [unit]	Value
ABS infill percentage	*inm* [1]	1.00
ABS component volume	*Vm* [cm^3]	85.54
ABS density	*ρm* [g/cm^3]	1.10
ABS cost	*Pm* [€/kg]	50.00
Breakaway infill percentage	*inms* [1]	0.1
Breakaway volume	*Vms* [cm^3]	1.01
Breakaway density	*ρms* [g/cm^3]	1.22
Breakaway cost	*Pms* [€/kg]	72.67
Material cost	*M* [€]	4.71

The cost of labour is 20.00 € per orthoses (Table 8). *Tl* included the scanning time, non-deposition times and a fraction of the deposition time since the continuous presence of the operator is unnecessary. *Pl* is a rough estimate and it is strongly dependent on the professional figure of the health care operator and the facility in which he operates.

Table 8. Labour parameters and cost.

Parameter	Symbol [unit]	Value
Labour time	*Tl* [h]	0.50
Labour wage	*Pl* [€/h]	40.00
Labour cost	*L* [€]	20.00

Combining P, S, E, M and L contributes, the total cost of a customized orthoses fabricated by means of AM results equal to 25.84 €. The analysis of the costs shows that the greater part of the orthotic fabrication cost is determined by the labour cost, accounting for 78% of the whole cost. The second most impactful parameter is material cost, representing 18% of the whole cost. Although the proposed approach requires dedicated equipment (high-speed and accurate 3D scanner, 3D printer and modelling software), the cost analysis highlights that this solution is competitive with respect to traditional customized orthoses. The total fabrication time (2.46 h) is given by the sum of the scanning acquisition, GUI modelling and 3D printing times. Time analysis shows that the most time-consuming phase is 3D printing, which lasts slightly more than two hours. Beyond that, the timing of the procedure proposed in the current study is compatible with the intended clinical practices: the treatment of non-emergency conditions affecting the joints and bones of the hand-wrist-arm district. In particular, the approach is advantageous with respect to vacuum forming, which may take up to several days owing to the negative and positive mould generation activities involved for fabricating a customized orthosis.

4. Conclusion

The present study was developed, proposing an alternative methodology to fabricate orthosis for the treatment of non-acute conditions of the hand-wrist-arm district via reverse engineering and additive manufacturing. The suggested methodology involved the design of a GUI, integrating a series of standardized and semi-automatic commands to support the healthcare operators in the modelling of the medical device.

The results of the analysis demonstrated the feasibility of the developed approach in terms of time and cost-effectiveness and, therefore, the viability of implementing the solution in clinical practice. An early prototype of the limb orthosis was printed using ABS by means of a desktop FDM machine. The proposed set-up ensured the fabrication of orthotic device even in healthcare facilities. The device cost was estimated to be around 26€, requiring 0.03 h, 0.23 h and 2.20 h for its scanning, modelling and printing phases, respectively.

Future works will provide further evidence on the appropriateness in terms of cost, time and mechanical behaviour of the proposed medical solution by conducting experimental analyses aimed at expanding the portfolio of biocompatible materials that can be used for 3D printing orthoses. Besides, further information on patient acceptance and clinical efficacy of the AM customized solutions should be investigated. Consideration should also be given to the aspect of comfort: specific solutions to promote wearability should be investigated (e.g., orthotic surface smoothing treatment or development of soft sleeves internal to the orthosis).

Acknowledgements

The author would like to acknowledge Dr. Gian Maria Marotti and DDX Software Solutions for their professional contribution in the development of the GUI during his Master Thesis.

References

[1] K. Chuen Wong, 3D-printed patient-specific applications in orthopedics, Orthop. Res. Rev. 8 (2016) 57–66. https://doi.org/10.2147/ORR.S99614.

[2] V. Vladinovskis, Review of 3D Printing Technologies and Considerations on Their Use in Orthopedy, 2020 IEEE 61st Annu. Int. Sci. Conf. Power Electr. Eng. Riga Tech. Univ. RTUCON 2020 - Proc. (2020). https://doi.org/10.1109/RTUCON51174.2020.9316483.

[3] J. Barrios-Muriel, F. Romero-Sánchez, F.J. Alonso-Sánchez, D.R. Salgado, Advances in Orthotic and Prosthetic Manufacturing: A Technology Review, Mater. (Basel, Switzerland). 13 (2020). https://doi.org/10.3390/MA13020295.

[4] A.M. Paterson, R. Bibb, R.I. Campbell, G. Bingham, Comparing additive manufacturing technologies for customised wrist splints, Undefined. 21 (2015) 230–243. https://doi.org/10.1108/RPJ-10-2013-0099.

[5] A.S. Boyd, H.J. Benjamin, C. Asplund, Principles of casting and splinting, Am. Fam. Physician. 79 (2009).

[6] M. Halanski, K.J. Noonan, Cast and splint immobilization: Complications, J. Am. Acad. Orthop. Surg. 16 (2008) 30–40. https://doi.org/10.5435/00124635-200801000-00005.

[7] F. Blaya, P.S. Pedro, J.L. Silva, R. D'Amato, E.S. Heras, J.A. Juanes, Design of an Orthopedic Product by Using Additive Manufacturing Technology: The Arm Splint, J. Med. Syst. 42 (2018). https://doi.org/10.1007/S10916-018-0909-6.

[8] G. Baronio, S. Harran, A. Signoroni, A Critical Analysis of a Hand Orthosis Reverse Engineering and 3D Printing Process, Appl. Bionics Biomech. 2016 (2016). https://doi.org/10.1155/2016/8347478.

[9] D. Palousek, J. Rosicky, D. Koutny, P. Stoklásek, T. Navrat, Pilot study of the wrist orthosis design process, Rapid Prototyp. J. 20 (2014) 27–32. https://doi.org/10.1108/RPJ-03-2012-0027.

[10] H. Kim, S. Jeong, Case study: Hybrid model for the customized wrist orthosis using 3D printing, J. Mech. Sci. Technol. 2015 2912. 29 (2015) 5151–5156. https://doi.org/10.1007/S12206-015-1115-9.

[11] ISO 10993-1:2018 - Biological evaluation of medical devices, (2020).

[12] S. Yim, D. Rosen, Build time and cost models for Additive Manufacturing process selection, Proc. ASME Des. Eng. Tech. Conf. 2 (2012) 375–382. https://doi.org/10.1115/DETC2012-70940.

[13] M. Ruffo, R. Hague, Cost estimation for rapid manufacturing - Simultaneous production of mixed components using laser sintering, Proc. Inst. Mech. Eng. Part B J. Eng. Manuf. 221 (2007) 1585–1591. https://doi.org/10.1243/09544054JEM894.

[14] ISO 6892-1:2020, Int. Stand. (2020).

[15] ISO 7438:2020 - Metallic materials - bend tests, Int. Stand. (2020).